^{101}Pd的能级结构研究以及与其邻近核素的系统性对比

Aman Rohilla　李广顺　王建国　柳敏良　周小红　郭松　强赞华　丁兵　侯东升　黄山

Structural Investigation in ^{101}Pd and Comparison in Its Vicinity

Aman Rohilla, LI Guangshun, WANG Jianguo, LIU Minliang, ZHOU Xiaohong, GUO Song, QIANG Yunhua, DING Bing, HOU Dongsheng, HUANG Shan

---

您可能感兴趣的其他文章

Articles you may be interested in

对关联在反磁转动中的作用（英文）

Effects of Pairing Correlations on the Antimagnetic Rotation

原子核物理评论. 2017, 34(1): 116−120　https://doi.org/10.11804/NuclPhysRev.34.01.116

丰中子锶同位素的投影壳模型研究

Projected Shell Model Studies for Neutron−rich Sr Isotopes

原子核物理评论. 2018, 35(1): 10−17　https://doi.org/10.11804/NuclPhysRev.35.01.010

Kr^{2+}辐照导致的Ca$_8$LnNa(PO$_4$)$_6$F$_2$(Ln=La,Nd和Sm)磷灰石结构陶瓷材料的非晶转变

Amorphization of Ca$_8$LnNa(PO$_4$)$_6$F$_2$(Ln=La, Nd and Sm) Apatite Ceramics Induced by Kr Ion Irradiation

原子核物理评论. 2019, 36(2): 224−229　https://doi.org/10.11804/NuclPhysRev.36.02.224

缺中子核素^{101}In低位同核异能态的首次观测

First Observation of the Low−lying Isomer State of ^{101}In

原子核物理评论. 2018, 35(4): 439−444　https://doi.org/10.11804/NuclPhysRev.35.04.439

RE2Ti$_2$O$_7$(RE=Gd,Y,Ho,Er)的结构、机械性能及热学性质的第一性原理研究(英文)

First−principles Study of Structural, Mechanical and Thermal Properties of RE$_2$Ti$_2$O$_7$ (RE=Gd, Y, Ho, Er)

原子核物理评论. 2019, 36(2): 248−255　https://doi.org/10.11804/NuclPhysRev.36.02.248

Er,Yb同位素链的基态形状(量子相)酷越研究(英文)

Ground State Shape (Phase) Crossover in Er and Yb Isotopes

原子核物理评论. 2019, 36(1): 43−48　https://doi.org/10.11804/NuclPhysRev.36.01.043

Structural Investigation in ^{101}Pd and Comparison in Its Vicinity

Aman Rohilla, LI Guangshun, WANG Jianguo, LIU Minliang†, ZHOU Xiaohong, GUO Song,

QIANG Yunhua, DING Bing, HOU Dongsheng, HUANG Shan

(*Institute of Modern Physics, Chinese Academy of Sciences, Lanzhou 730000, China*)

Abstract: The present work aims at the structural investigation of the $\gamma-$ levels in $\nu h_{11/2}$ band of ^{101}Pd, and its comparison with the neighboring Pd-isotopes. Theoretical investigations performed in the vicinity of Pd-isotopes *i.e.*, around $N=Z=50$ shell closures have described the systematic well, indicating an evolution of shape alongwith involvement of triaxiality. The deformation studies in the vicinity of Pd-isotopes around shell closures have predicted the shape change from small deformation to more deformed prolate shapes. The comparison of Total Routhian Surface (TRS) calculations performed in the present work have also suggested the inclusion of small amount of triaxiality as a function of increasing rotational frequency and neutron number, pointing towrads the $\gamma-$ softness present in the nuclei.

Key words: Pd-isotopes; $R_{4/2}$ (E_{4^+}/E_{2^+}); deformation; antimagnetic rotation; shears mechanism

1 Introduction

The variety of band structures have been observed experimentally in the vicinity of $N=Z=50$ shell closures, resulted from the coupling of valence nucleons with different shape driving effects and core-excited configurations[1–2]. Also, a number of bands have been observed in $A\sim 100$ mass region for the weakly deformed nuclei, within the framework of shears mechanism[3–5]. Other than this, new nuclear phenomena have been visualized at proton and neutron shell closures like: anti-magnetic (AMR) rotation[6–9], and band termination[5] at high spins in $^{98-100}$Ru[10], $^{101-102}$Rh[11–12], $^{98-100,102-103}$Pd[13–23], and ^{98,99}Ag[24–25] nuclei. These different band structures with varying trends of moment of inertia and reduced transition probabilities as a function of increasing rotational spin are exhibited to have large angular momentum based on different geometrical configurations[3]. Also, the observation of slower decrease of B(E2) values in ^{110}Cd compared to that in pure AMR bands in ^{106,108}Cd isotopes have evidenced for the interplay between antimagnetic and core rotation[26].

For the aforementioned nuclei, the antimagnetic rotation bands based on $g_{9/2}^{-2}$ configurations have been identified and reported in the literature on the basis of lifetime measurements performed using Doppler Shift Attenuation Method (DSAM) method[21]. And, it will be interesting to investigate the evolution of triaxiality and the effect of weakly deformed core on AMR character in Pd-isotopes. For this purpose, we have performed the theoretical investigations in the neighboring Pd-nuclei around $N=Z=50$ shell closures.

In the present work, a study of structural changes have been reported based on: (a) DSAM measured lifetimes present in the literature, and (b) theroretical investigations around $N=Z=50$ shell closures. This paper has been organized as follows: Firstly, the discussion about the experimental considerations reported in literature has been made based on DSAM procedure, and the related necessary key details for such a method have been made in Section 2. Also, the importance of target (with and without backing) for DSAM measurement has been discuused. Secondly, the discussion of results have been made in Section 3, based on the comparison of experimental data available in the literature with theoretical investigations performed in the present work, for nuclei with $Z \sim 46$. Lastly in Section 4, summary and conclusion have been given.

2   Experimental considerations

The high spin states in ^{101}Pd had been popu-lated via different nuclear reactions presented in the Refs. [20−21]. Both of the reactions had been used to populate the excited states in ^{101}Pd nuclei consider-ing different experimental procedures, mainly focus-ing on measuring the lineshapes of the excited states based on DSAM method. The detailed consideration relevant to experimental procedures could be found in the Refs. [20−21]. The main point to discuss here is the different type of backings used in those two exper-iments for DSAM measurements. In one of the refer-ence, self supporting but thick target has been used for reaction, of which some part is used as an effect-ive target area and remaining part is used as an ef-fective stopping area[20]. While in the Ref. [21], backed target with required thickness of backing was used to populate the states in ^{101}Pd nuclei. So, the key im-portance of using the target with backing and without backing has been discussed for successfully carrying out of a DSAM measurement.

To carry out DSAM based lineshape measure-ment, it is required to have backing with large thick-ness of order $\sim (8 \sim 10)$ mg/cm^2 *i.e.*, the backing must be thick enough to stop the residuals/recoils in-side it. The stopping of the residuals produces the ve-locity profile in the backing assuming the negligible energy loss in target, and thus produce the lineshapes required for extracting lifetimes employing LINESHAPE program[27]. For lineshape analysis, data obtained at detectors placed at an angle were sorted and added together to obtain an angle dependent $\gamma-$ray spectrum. Then, the $\gamma - \gamma$ coincidence events were sorted into three asymmetric matrices, whose $x-$axis was the $\gamma-$ ray energies in the detectors placed at the same angle, while the $y-$axis for these matrices was the $\gamma-$ ray energies in the detectors placed at other position. For the purpose of experimental dis-cussion, level scheme shown in Fig. 1(a) has been taken from the Ref. [21].
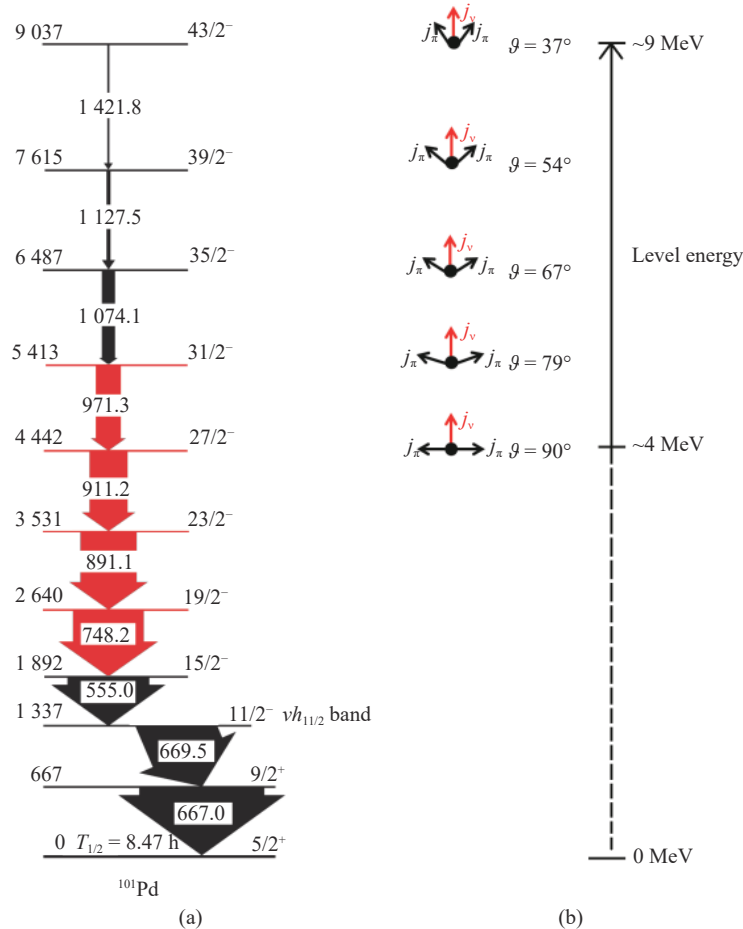

Fig. 1   (color online)(a) The reproduced partial level scheme relevant for the present work has been taken from the Ref. [21]. In figure (b), the pictorial representation for the generation of angular momentum has been shown as a func-tion of increasing level energy and spin of the level states, in $\nu h_{11/2}$ band of ^{101}Pd. The ϑ values in between the proton and neutron blades have been also taken from the Ref. [21].

3　Discussion

The observed antimagnetic rotational bands[3, 28] in the last decades have shown a regular rotational behavior, despite of the nuclei small deformation. This has been resulted into the production of high spin excited states, with proton states more and more aligned along the neutron aligned states *i.e.*, rotation axis. This type of alignment has resulted in an increase of angular momentum, due to the coupling of proton and neutron aligned states, known as shears mechanism, which can be seen in the pictorial representation (see Fig. 1(b)). To validate this pictorial behavior, the experimentally measured B(E2) values[29–30] are plotted and compared as a function of increasing spin. The comparison has suggested the observation of B(E2) values for ^{101}Pd in between those observed for ^{100}Pd and ^{102}Pd nuclei. Other than this, the decreasing behavior of B(E2) values have been seen with increasing spin. This behavior can be characterized from the appearance of weak E2 transitions reflecting the weakly deformed core, which is one of the key factor for indication of required antimagnetic rotation character in lower part of $\nu h_{11/2}$ band[21]. This type of decreasing trend, suggesting the AMR behavior in $\nu h_{11/2}$ band was also supported theoretically[20], based on semi-classical model (Refs. [17–19] of Ref. [20]). Also, the theoretical studies for AMR bands in Pd isotopes, based on particle rotor model (PRM) and tilted-axis craking (TAC) shell model[31–22] have inferred the $\pi g_{9/2}^{-4}$ based configuration for the AMR band, within the framework of PRM. However, Refs. [18, 21, 31] have favored the $\pi g_{9/2}^{-2}$ based configuration based on TAC and PRM calculations. The observed decreasing B(E2) values and the generated angular momentum in the neighboring nuclei, can be suggested due to the evolution of vibrational picture at lower spins, to a more rotor-like picture at higher spins[32] around $23/2^-$ due to the alignment of presumably $g_{7/2}$ neutrons. This change is likely to be predicted due to configuration change of the band above $23/2^-$, having an impact on the measured lifetime values and the extracted B(E2) values above this level.

To check the evolution of deformation as a function of neutron number for Pd-isotopes, β_2 values taken from the Ref. [33] are plotted (shown in the Fig. 2). This has been done to observe the trend of deformation in Pd-isotopes and the neighboring nuclei around $N=Z=50$ shell closures. From the graph plotted for isobars ($A=101$) and isotones ($N=55$), in vicinity of $Z=46$, the change in shape has been observed with increasing proton number. The large prolate deforma-

tion with $\beta_2 \sim 0.2$ has been observed at $Z=44$ with continuous decrease and reaching to small oblate deformation value at shell closures. Beyond $Z=50$, the large increase in deformation has been observed for $N=55$ isotones with small increase in deformation for isobars ($A=101$). The reason for this large increase of β_2 can be given due to the occupancy of more deformation driving orbital resulting in increasing prolate deformation for $N=55$ isotones. For Pd- isotopes plotted with increasing neutron number (Fig. 2), nearly spherical shapes have been observed with small value of deformation for $N=48$ to 52. Thereafter, a continuous rise in deformation has been observed, suggesting the inclusion of more prolate deformation driving orbital above $N=52$. These two types of comparisons around $N=Z=50$ have been done to check: (1) the effect of extra neutron or proton towards deformation and spherecity, and (2) at which neutron or proton number above or below Pd-nuclei, the transition of nuclear shape takes place. This check further provides the verification for one of the characteristics of nuclei lying in transitional region of $A\sim100$.
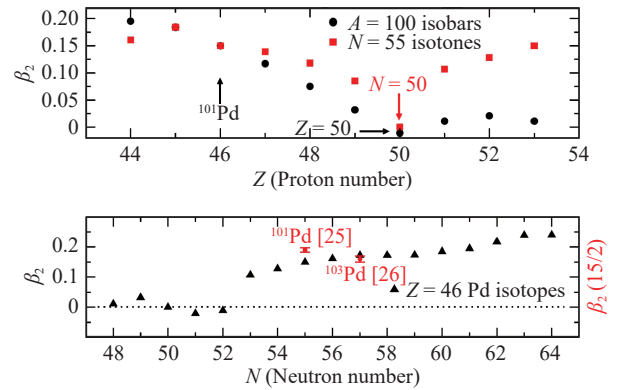

Fig. 2　(color online)The deformation (same scaling has been used on left as well as right of $y-$ axis) is plotted with increasing neutron number for Pd-isotopes (lower). In the upper figure, the deformation is plotted in the vicinity of $N=Z=50$ shell closures. The deformation values are taken from the Atomic Data and Nuclear Tables 2016[33]. The experimentally observed β_2 values for ^{101}Pd and ^{103}Pd for the $15/2^-$ state are taken from the Refs. [34–35] respectively.

To visualize the nature of shape evolution around Pd-isotopes, the ratios of E_{4+}/E_{2+}[36–37] have been calculated, which is one of the experimental signature of spherical and defromed shape in nuclei as suggested by casten triangle[37]. In the present case, smooth change of this ratio has been observed from 2.1 onwards, as a funciton of increasing neutron number (see Fig. 3), indicating the shape evolution from a spherical nucleus towards $\gamma-$ soft triaxial rotor with involvement of small triaxiality (γ). The deformation para-

meter (γ) measures the degree of triaxiality. The $(\gamma = 0°)$ limit corresponds to axial prolate shapes $(\beta_2 > 0)$ while oblate axial shapes $(\beta_2 < 0)$ appear at $(\gamma = 60°)$. Intermediate values of $\gamma-$ are associated with triaxial shapes[36–37]. This is futher supported by the performed TRS calculations presented in Ref. [34].
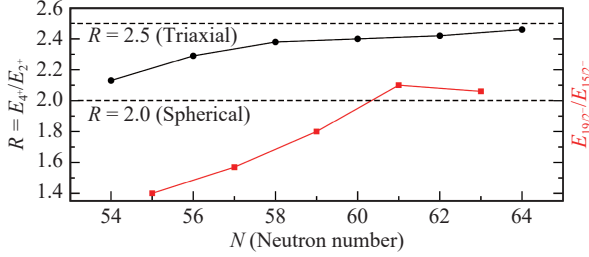

Fig. 3   (color online)The ratio of E_4^+/E_2^+ (scaled on left of $y-$axis) are plotted with increasing neutron number for even-A Pd-isotopes (black color) and $E_{19/2^-}/E_{15/2^-}$ (scaled on right of $y-$axis) for odd-A Pd-isotopes (red color)[38]. On both sides of the figure, same scaling has been used as labelled on left of $y-$axis.

To get the deeper understanding about the shape of nucleus, we have performed the Total Routhian Surface (TRS) Calculations, within the Cranked Hartree-Fock-Bogoliubov (CHFB) model[39–40]. Collective rotation was investigated in the frame of the cranked shell model in three-dimensional deformation space comprising of β_2, β_4 and γ nuclear shape parameters. The paraemeters used in TRS measurement have their usual meaning *i.e.*, β_2 is quadrupole deformation, β_4 is hexadecapole deformation and γ is the triaxiality present in the nucleus. The detailed information about the performed TRS calculations can be found in the Refs. [40–43] and the references therein. Pairing correlations are dependent on the rotational frequency and deformation. In order to study this, the TRS calculations have been carried out in deformation space for $^{100-102}$Pd, paying an attention to the evolution of $\gamma-$softness and triaxiality with rotation. At a given frequency, the deformation of a state was determined by minimizing the calculated TRS. The calculated equilibrium deformation indicates that our calculations are in close agreement to some extent with the results already reported in the literature. The shape evolution and nuclear softness in β_2 and γ directions are evaluated as shown in Fig. 4. The performed TRS calculations in the present work only picturizes the presence of triaxaility at higher excitations in terms of rotational frequency. On comparison of the present TRS results with the calucaltions reported in literature have predicted energy minima at $(\beta_2, \gamma) = (0.133, 1.2°)$[34] for ^{100}Pd, $(0.165, 10.0°)$ for ^{101}Pd (present work), and $(0.160, 6.2°)$ for ^{102}Pd[16]

nuclei, have also confirmed the involvement of triaxiality with change in neutron number. This can be seen from the magnitude of triaxiality paramter (γ) value mentioned in the parenthesis above. From the above mentioned results based on $R_{4/2}$ and TRS measurements, shape change from vibration to rotation has been described including the small amount of triaxiality, and the effects like: rotation-vibration coupling in Pd-isotopes and in its vicinity *i.e.*, $N = 50$ shell closures.
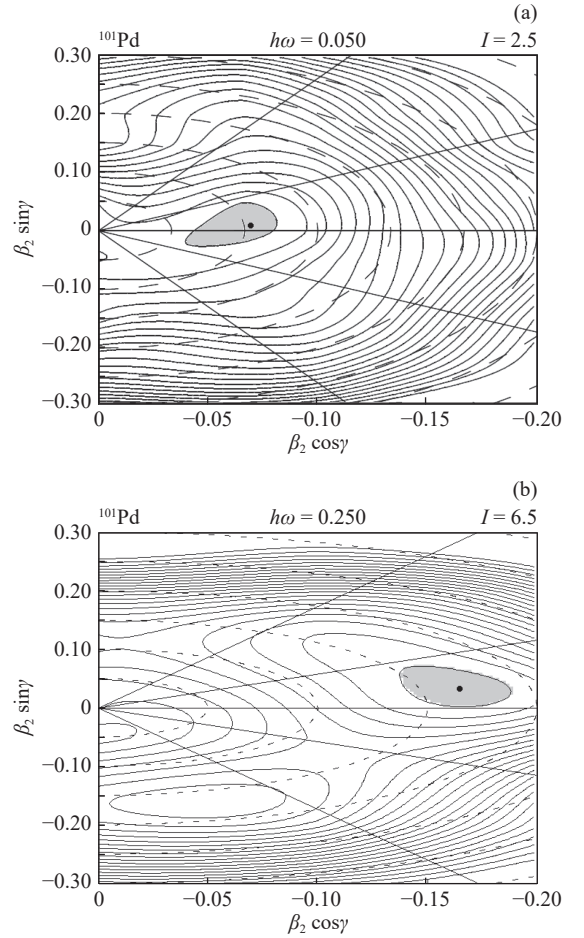

Fig. 4   TRS calculations for ^{101}Pd nuclei at $h\omega = 0.050$ (a) & 0.250 (b) MeV are shown. The parameters at the minimum energy were $(\beta_2, \gamma) = (0.065, 4°)$ and $(0.165, 10°)$ at 0.050, 0.250 MeV energy respectively.

4   Summary and conclusions

In this paper, structural change based on DSAM investigated lifetimes for some of the excited states in $\nu h_{11/2}$ band of ^{101}Pd are presented. The decreasing behavior of extracted transitional probabilities have been observed as a function of increasing spin from the reproted experimental considerations in the literature, indicating antimagnetic rotation in $\nu h_{11/2}$ band. The deformation studies in the vicinity of Pd-

isotopes around $N=Z=50$ shell closures have predicted the shape change from small deformation to more deformed prolate shapes. The TRS calculations presented in this manuscript for ^{100}Pd, ^{101}Pd and ^{102}Pd have suggested the involvement of triaxiality, which is further supported by the E_{4+}/E_{2+} ratio. Also, more theoretical calculations are still needed to study the transition from $U(5)$ to $O(6)$ behavior based on interacting boson model and triaxial projected shell model, to confirm the evolution of triaxiality in Pd-isotopes, and for strongly supporting the already reported antimagnetic character.

References:

[1] REVIOL W, GARGA U, AHMADB I, et al. Nucl Phys A, 1993, 557: 391.

[2] ERTOPRAK A, CEDERWALL B, QI C, et al. Eur Phys J A, 2018, 54: 145.

[3] FRAUENDORF S. Rev Mod Phys, 2001, 73: 463.

[4] CLARK R M, ASZTALOS S J, BUSSE B, et al. Phys Rev Lett, 1999, 82: 3220; CLARK R M, MACCHIAVELLI A O. Nucl Phys A, 2001, 682: 415.

[5] SIMONS A J, WADSWORTH R, JENKINS D G , et al. Phys Rev Lett, 2003, 91: 162501.

[6] HE C Y, ZHU L H, WU X G，et al. Phys Rev C, 2010, 81: 057301.

[7] YAO S H, MA H L, ZHU L H, et al. Phys Rev C, 2014, 89: 014327.

[8] HE C Y. Nucl Phys A, 2010, 834: 84c.

[9] WANG M,WANG Y Y, ZHU L H, et al. Phys Rev C, 2018, 98: 014304.

[10] TIMÁR J, GIZON J, GIZON A, et al. Phys Rev C, 2000, 62: 044317.

[11] TIMÁR J, GIZON J, GIZON A, et al. Euro Phys J A, 1999, 4: 11.

[12] GIZON J, CĂTA-DANIL G, GIZON A, et al. Phys Rev C, 1998, 59: R570(R).

[13] CEDERKĂLL J, PEREZ G, LIPOGLAVŠEK M, et al. Z Phys A Hadrons Nucl, 1997, 359: 227.

[14] SIHOTRA S, NAIKZ, KUMAR S, et al. Phys Rev C, 2011, 83: 024313.

[15] PEREZ G E, SOHLERA D, ALGORA A, et al. Nucl Phys A, 2001, 686: 41.

[16] GIZON J, NYAKÓ B M, TIMÁR J, et al. Phys Lett B, 1997, 410: 95.

[17] NYAKÓ B M, GIZON J, GIZON A, et al. Phys Rev C, 1999, 60: 024307.

[18] SINGH V, SIHOTRA S, BHAT G H, et al. Phys Rev C, 2017, 95: 064312.

[19] ZHU S, GARG U, AFANASJEV A V, et al. Phys Rev C, 2001, 64: 041302.

[20] SUGWARA M, HAYAKAWA T, OSHIMA M, et al. Phys Rev C, 2015, 92: 024309.

[21] SINGH V, HAYAKAWA T, M OSHIMA, et al. Jour Phys G: Nucl Part Phys, 2017, 44: 075105.

[22] RATHER N, ROY S, DATTA P, et al. Phys Rev C, 2014, 89: 061303.

[23] MA K Y, LU J B, LI J, et al. Phys Rev C, 2019, 100: 014326.

[24] CEDERKÄLL J, LIPOGLAVŠEK M, PALACZ M, et al. Euro Phys J A, 1998, 1: 7.

[25] SOHLER D, DOMBRÁDI Z, BLOMQVIST J, et al. Euro Phys J A, 2003, 16: 171.

[26] ROY S, CHATTOPADHYAY S, DATTA P, et al. Phys Lett B, 2011, 694: 322.

[27] WELLS J C, JOHNSON N R. ORNL Physics Division Prog Rep No. ORNL-668944[EB/OL].[2019-12-10]. https://personalpages.manchester.ac.uk/staff/dave.cullen/lineshapes.pdf.

[28] CLARK R M, MACCHIAVELLI A O, et al. Annu Rev Nucl Part Sci, 2000, 50: 1.

[29] RADECK D, BLAZHEV A, ALBERS M, et al. Phys Rev C, 2009, 80: 044331.

[30] AYANGEAKAA A D, GARG U, CAPRIO M A, et al. Phys Rev Lett, 2013, 110: 102501.

[31] JIA H, QI B, LIU C, et al. Phys Rev C, 2018, 97: 024335.

[32] REGAN P H, BEAUSANG C W, ZAMFIR N V, et al. Phys Rev Lett, 2003, 90: 152502.

[33] MÖLLER P, SIERKA A J, ICHIKAW T, et al. At and Nucl Data Tab, 2016, 109-110: 1.

[34] ANAGNOSTATOU V, REGAN P H, WERNER V, et al. App Rad and Iso, 2012, 70: 1321.

[35] ASHLEY S F, REGAN P H,ANDGREN K, et al. Phys Rev C, 2007, 76: 064302.

[36] ZAMFIR N V, CASTEN R F. Phys Lett B, 1993, 305: 317.

[37] CASTEN R F. Nature Physics, 2006, 2: 811.

[38] National Nuclear Data Center[EB/OL].[2019-12-10]. https://nndc.bnl.gov/nudat2/.

[39] NAZAREWICZ W, RILEY M A, GARRETTE J D, et al. Nucl Phys A, 1990, 512: 61.

[40] NAZAREWICZ W, DUDEK J, BENGTSSON R, et al. Nucl Phys A, 1985, 435: 397.

[41] SATULA W, WYSS R, MAGIERSKI P, et al. Nucl Phys A, 1994, 578: 45.

[42] ROHILLA A, GUPTA C K, SINGH R P, et al. Eur Phys Jour A, 2017, 53: 64.

[43] ROHILLA A, SINGH R P, MURALITHAR S, et al. Phys Rev C, 2019, 100: 024325.

^{101}Pd 的能级结构研究以及与其邻近核素的系统性对比

Aman Rohilla, 李广顺, 王建国, 柳敏良†, 周小红, 郭 松, 强赟华, 丁 兵, 侯东升, 黄 山

(中国科学院近代物理研究所，兰州　730000)

摘要：　在本工作中，我们主要研究了 ^{101}Pd 核中 $\nu_{11/2}$ 带的能级结构，并与临近同位素相对应的能级结构进行了对比。研究发现在 Pd 同位素链，即 $N=Z=50$ 的壳附近，三轴形变的演变符合很好的系统性，即从小的不稳定形变逐渐演变为稳定的长椭形变。同时，我们也做了总势能面 (TRS) 随着原子核转动频率以及中子数变化的系统计算，结果也支持该核区不稳定三轴形变演化的规律。

关键词：　Pd 同位素链；$R_{4/2}$ (E_4^+/E_2^+)；形变；反磁转动；剪刀机制